Power-Domain Impedance Theory for the Analysis and Mitigation of Interarea Oscillations

Shahil Shah¹, Weihang Yan¹, Vahan Gevorgian¹, and Wenzhong Gao²

¹National Renewable Energy Laboratory (NREL) Golden, CO 80401, USA

Email: {Shahil.Shah, Weihang.Yan, Vahan.Gevorgian}@nrel.gov

²University of Denver Denver, CO 80208, USA Email: Wenzhong.Gao@du.edu

Abstract—This paper presents an impedance-based theory for the analysis and mitigation of interarea oscillations in power systems. Because low-frequency power system oscillations primarily manifest in phasor quantities, including active and reactive power flows, and the magnitude and frequency of bus voltages, a new-type of impedance, called power-domain impedance, is defined in terms of these phasor quantities. The power-domain impedance provides an intuitive framework for the analysis of interarea oscillations without requiring internal details of generators, and it is ideally suited for developing oscillation damping controls in inverter-based resources. The power-domain impedance theory is demonstrated in this paper using PSCAD simulations of a two-area system. The theory is also used for designing damping control in synchronous generators and a wind power plant in the two-area system.

Index Terms—Power system oscillations, interarea modes, impedance analysis, wind power plants, damping.

I. INTRODUCTION

Power system oscillations triggered by disturbances such as generation outages or transmission line faults can result in system separation because of large swings in the active power flow over intertie lines, potentially leading to a major blackout event [1]-[5]. It is critical for the reliable operation of a power system that its interarea oscillation modes remain sufficiently damped under all resource dispatch scenarios. Usually the interarea modes are damped by installing power system stabilizers (PSS) in the control system of synchronous generators [6], [7]; however, there is a growing concern that the displacement of synchronous generation by inverter-based resources (IBR) may negatively impact the damping of the interarea modes. For example, a recent study by ERCOT showed that it will be important for IBR to provide PSStype damping for the reliable operation of the Texas Interconnection as the IBR penetration increases to higher levels [8], [9]. Implementing the PSS functionality in IBR will require new analytical tools because the existing approaches for the analysis of interarea oscillations rely on high fidelity models of generators,

which are seldom available for IBR—manufacturers do not disclose internal details of inverters, wind turbines, etc., because such details are considered proprietary. The objective of this paper is to develop a measurement-based method for the analysis of interarea oscillations that can support the PSS design for both synchronous generators and IBR without requiring dynamic models.

State-space modal analysis is the standard technique for the evaluation of power system oscillation modes. Modal analysis is also used to quantify the participation of generators in a particular interarea mode and identify generators where PSS installation will be the most effective in damping the mode [6]. The state-space analysis, however, requires accurate models of generating resources; hence, its applicability is limited for designing the PSS functionality in IBR. In contrast to the modal analysis, Prony analysis is a measurement-based method for the analysis of power system oscillations [10]. It basically involves the identification of the frequency, damping, and phase of the oscillation modes using time-domain responses of different quantities following a transient event. The Prony method, however, does not provide much insight for designing the PSS functionality in generators and IBR.

Impedance-based approach is increasingly becoming the mainstream tool for conducting stability evaluation of converter-based power systems such as wind and PV power plants, and HVDC transmission networks [11], [12]. This paper adapts the impedance approach for the analysis of interarea oscillations by defining a new type of impedance, called power-domain impedance. The power-domain impedance responses can be measured by IBR for the online monitoring of the frequency and damping of the power system oscillation modes. The proposed power-domain impedance-based analysis of interarea oscillations is demonstrated on a modified Kundur's two-area system. It is also used to design the PSS functionality in synchronous generators and a wind power plant in the two-area system.

II. POWER-DOMAIN IMPEDANCE THEORY

A. Impedance-Based Stability Analysis

Fig. 1 shows Kundur's two-area system used in this paper to demonstrate the impedance-based analysis of interarea oscillations [6]. As shown in Fig. 1, the system is partitioned into two subsystems for impedance-based stability analysis; the impedances of the partitioned subsystems are denoted by $\mathbf{Z}_1(s)$ and $\mathbf{Z}_2(s)$, respectively. Bold letters are used because the impedance response of a three-phase network is a two-by-two transfer matrix irrespective of the domain in which the impedance is defined [11].

This work was authored by Alliance for Sustainable Energy, LLC, the manager and operator of the National Renewable Energy Laboratory for the U.S. Department of Energy (DOE) under Contract No. DE-AC36-08GO28308. Funding provided by U.S. Department of Energy Office of Energy Efficiency and Renewable Energy Wind Energy Technologies Office. The views expressed in the article do not necessarily represent the views of the DOE or the U.S. Government. The U.S. Government retains and the publisher, by accepting the article for publication, acknowledges that the U.S. Government retains a nonexclusive, paid-up, irrevocable, worldwide license to publish or reproduce the published form of this work, or allow others to do so, for U.S. Government purposes.

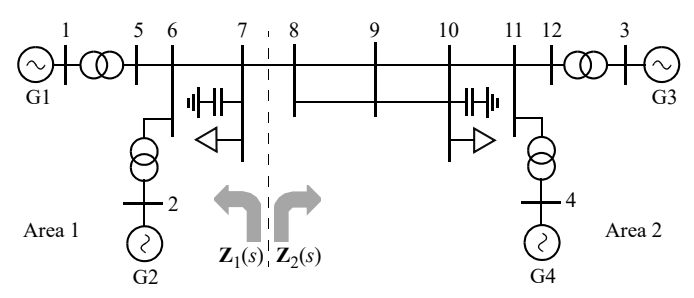


Fig. 1. Modified Kundur's two-area system.

Based on the impedance analysis theory, the characteristic equation of the system is given by [12]:

$$\mathbf{I} + \mathbf{Z}_1(s) \cdot \mathbf{Z}_2(s)^{-1} = \mathbf{0} \tag{1}$$

System stability analysis can be performed by applying the generalized Nyquist criteria to the impedance-ratio matrix $\mathbf{Z}_1(s) \cdot \mathbf{Z}_2(s)^{-1}$. To apply the Nyquist criteria, we first need to know the number of right-half plane poles (RHP) in the impedance-ratio matrix. Note that the number of RHP in the ratio matrix is equal to the sum of the number of RHP in $\mathbb{Z}_1(s)$ and the number of right-half plane zeros (RHZ) in $\mathbb{Z}_2(s)$. We make an assumption that the two subsystems are individually stable; this assumption implies that $\mathbf{Z}_1(s)$ and $\mathbf{Z}_2(s)$ do not have any RHP [12]. Because the number of RHP in $\mathbb{Z}_2(s)$ is zero, the number of RHZ in $\mathbb{Z}_2(s)$ can be obtained by counting the encirclements of origin by its Nyquist plot. If the total number of RHP in the impedance-ratio matrix is found as P and the number of encirclements of the critical point $(-1+i\cdot0)$ by the eigenvalues of the impedance-ratio matrix is N, then the number of RHP of the twoarea system, Z, is given by X = N + P; obviously, X must be zero for the two-area system to be stable. In most practical case there are no RHZ in $\mathbb{Z}_2(s)$, and hence, P is zero; for such cases, system stability can be ascertained simply by noting if the Nyquist plots of the eigenvalues of the impedance-ratio matrix, $\mathbf{Z}_1(s) \cdot \mathbf{Z}_2(s)^{-1}$, encircle the critical point or not. Note that the above discussion is valid irrespective of the domain in which $\mathbf{Z}_1(s)$ and $\mathbf{Z}_2(s)$ are defined [11].

B. Power-Domain Impedance

The impedances $\mathbf{Z}_1(s)$ and $\mathbf{Z}_2(s)$ can be represented either in the dq, sequence, or phasor domain [11]. However, power system oscillations are mainly governed by slow governor and exciter control functions of generators and their mechanical dynamics; hence, these oscillations manifest primarily in the phasor quantities including active and reactive power flows, and the magnitude and frequency of bus voltages [6]. It is much more insightful if the analysis of power system oscillations deals directly with these phasor quantities instead of instantaneous voltages and currents—the reason why the small-signal modal analysis uses active and reactive power flows, and frequencies (or angles) and magnitudes of bus voltages as state variables [6]. Hence, for the impedance-based analysis of interarea oscillations, a new type of impedance is defined in this paper relating the active and reactive power flows with the frequency and magnitude of the voltages at the terminals of a three-phase network:



Fig. 2. Block-diagram showing the flow perturbations in active and reactive power flows and the magnitude and frequency of voltages at the point of interconnection between two power system areas.

$$\begin{bmatrix} F(s) \\ V_m(s) \end{bmatrix} = \begin{bmatrix} Z_{\text{FP}}(s) & Z_{\text{FQ}}(s) \\ Z_{\text{VP}}(s) & Z_{\text{VQ}}(s) \end{bmatrix} \begin{bmatrix} P(s) \\ Q(s) \end{bmatrix}$$
(2)

where P(s) and Q(s) represent small-signal perturbation in the active and reactive power inputs of the network, respectively, and F(s) and $V_m(s)$ represent small-signal perturbation in the frequency and magnitude of the three-phase voltages at the terminals of the network. The two-by-two matrix in (2) maps the perturbation in the active and reactive power inputs of a network to the frequency and magnitude of voltages at its terminals. It is termed as power-domain impedance and denoted as \mathbf{Z}_{POWER} . For clarity, in the rest of the paper, the term "POWER" is dropped from the subscript; however, note that all impedances in this paper are defined in the "power-domain".

The flow of perturbations between the two partitioned subsystems of Fig. 1 can be described by a feedback loop as shown in Fig. 2. It is evident from Fig. 2 that the loop gain of the two-area system can be written as $\mathbf{Z}_1(s) \cdot \mathbf{Z}_2(s)^{-1}$, and system stability analysis can be performed by applying the generalized Nyquist criteria to this impedance-ratio matrix.

The power-domain impedance of a network can be measured by injecting perturbations in the active and reactive power input of the network and measuring the response in the frequency and magnitude of the voltages at the point of interconnection. Because the frequency of interarea oscillations is generally less than a couple of hertz, the power-domain impedances need to be measured only up to a few hertz. Most IBR, such as PV or storage inverters and wind turbines, can be programmed to inject active and reactive power perturbation at frequencies up to few hertz; hence, they can be used to obtain the power-domain impedance responses. Because one set of perturbation will give only two equations using (2) and we need to obtain four elements of the power-domain impedance, similar to the dq impedance measurement, two sets of linearly independent perturbations are required for measuring the power-domain impedance response.

C. Coupling in the Power-Domain Impedance

The frequency in power system is strongly coupled with the active power flows, and the voltage magnitudes are strongly coupled with the reactive power flows. Hence, it is expected that the off-diagonal elements of the power-domain impedance in (2) will be comparatively much smaller than the diagonal elements, at least at very low frequencies, where the steady-state droop characteristics dominate the impedance response. Moreover, power system oscillations are predominantly visible in the frequency and active power flows in comparison to voltages and reactive power

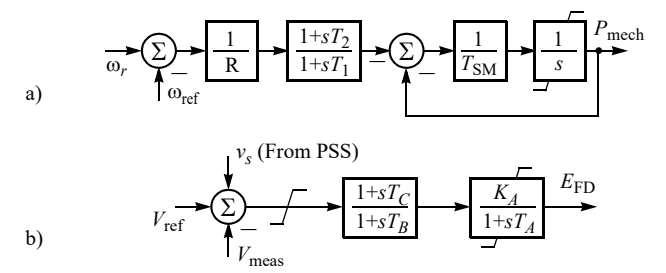


Fig. 3. Governor (TGOV4) and excitation system (AC4A) used in synchronous generators in the two-area system.

flows [2]. Hence, it can be expected that power system oscillations can be analyzed using only the first diagonal element of the power-domain impedance, $Z_{\rm FP}(s)$, relating the frequency with the active power input of a network. Nonetheless, note that coupling from the reactive power input to the frequency, $Z_{\rm FQ}(s)$, and from the active power input to the voltage magnitude, $Z_{\rm VP}(s)$, may not be negligible for all perturbation frequencies of interest; in fact, the PSS leverages this coupling by modulating the active power output of a generator through its excitation control to damp the oscillation modes of the system.

III. ANALYSIS OF INTERAREA OSCILLATIONS

A. Interarea Modes in a Two-Area System

This section applies the power-domain impedance method for the analysis of interarea oscillations in the Kundur's two-area system shown in Fig. 1. A 10 MW battery energy storage system (not shown in Fig. 1) is used for independently injecting active and reactive power perturbations to measure the power-domain impedance response. Fig. 3 shows the governor and excitation system used in all the generators. The PSS is disabled for the base-case presented in this subsection by fixing v_s in Fig. 3b) to zero.

Fig. 4 shows the measured responses of $\mathbb{Z}_1(s)$ and $\mathbb{Z}_2(s)$. Although the coupling $Z_{VP}(s)$ is much smaller than the diagonal element $Z_{VO}(s)$, the coupling from the reactive power to the frequency, $Z_{FO}(s)$, is nearly as strong as the diagonal element $Z_{FP}(s)$ in the frequency range shown in Fig. 4. This shows that the coupling from the reactive power to the frequency may play a significant role in power system oscillations, and it cannot be ignored in general. On the other hand, if both the off-diagonal elements are negligible, the analysis of interarea oscillations can be carried out simply by using the responses of the $Z_{FP}(s)$ element of $\mathbf{Z}_1(s)$ and $\mathbf{Z}_2(s)$. As shown in Fig. 4, the responses of $Z_{FP}(s)$ elements of both the areas intersect at 0.75 Hz with the phase margin of 12° (=180°-168°). Hence, power-domain impedance analysis ignoring the coupling effects predicts an under-damped interarea mode at 0.76 Hz. Fig. 5 shows the Nyquist plot of the eigenvalues of $\mathbf{Z}_1(s) \cdot \mathbf{Z}_2(s)^{-1}$, both considering and ignoring the coupling elements. Note from Fig. 5 that the analysis considering the coupling elements predicts an interarea mode also at around 0.75 Hz, albeit with a lower phase margin of 8.9°. Simulated response in Fig. 6 using PSCAD indeed confirm an under-damped interarea mode at around 0.75 Hz.

B. Damping by Synchronous Generators

The power-domain impedance method provides an intuitive

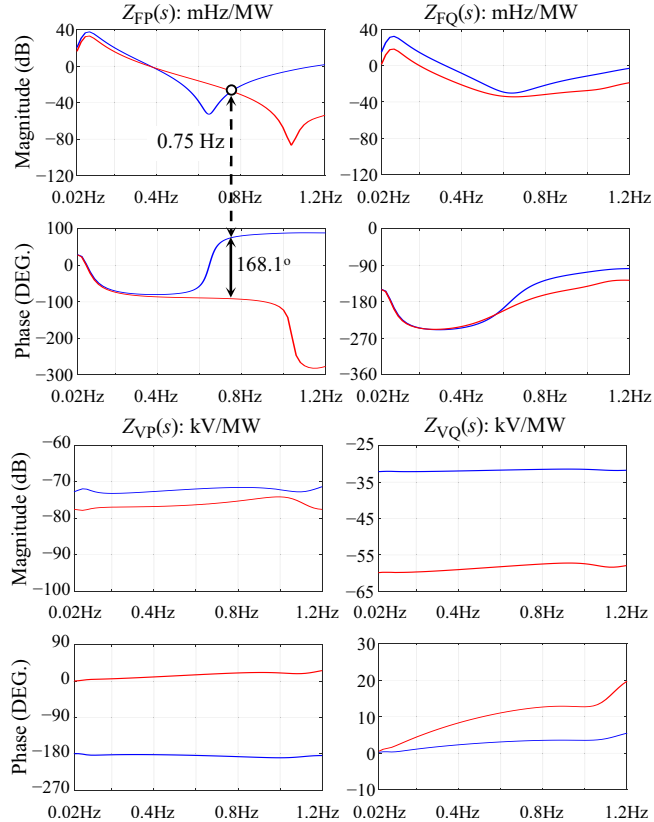


Fig. 4. Measured responses of the power-domain impedances $\mathbf{Z}_1(s)$, shown by red lines, and $\mathbf{Z}_2(s)$, shown by blue lines.

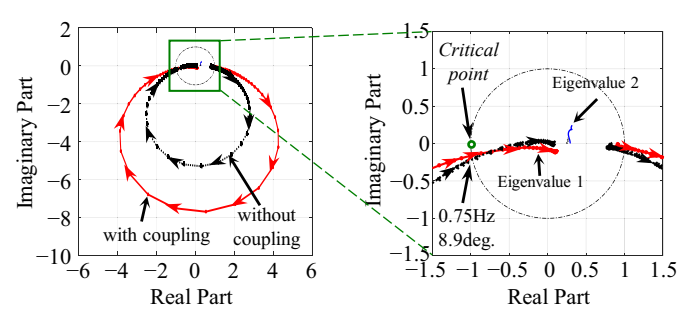


Fig. 5. Nyquist plot of the eigenvalues of the impedance-ratio matrix, $\mathbf{Z}_1(s) \cdot \mathbf{Z}_2(s)^{-1}$ (red solid lines). Nyquist plot of the eigenvalues ignoring coupling elements, i.e., assuming the off-diagonal elements of $\mathbf{Z}_1(s)$ and $\mathbf{Z}_2(s)$ are zero, is also shown (black dashed lines) for comparison.

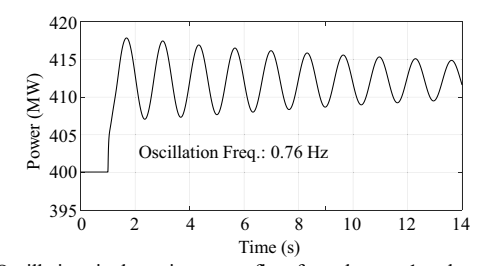


Fig. 6. Oscillations in the active power flow from the area 1 to the area 2 following a 30-MW load transient at 1 s.

framework for the control design of generators for damping the interarea oscillation modes. Fig. 7 shows the power-domain impedance analysis of the two-area system after the governor

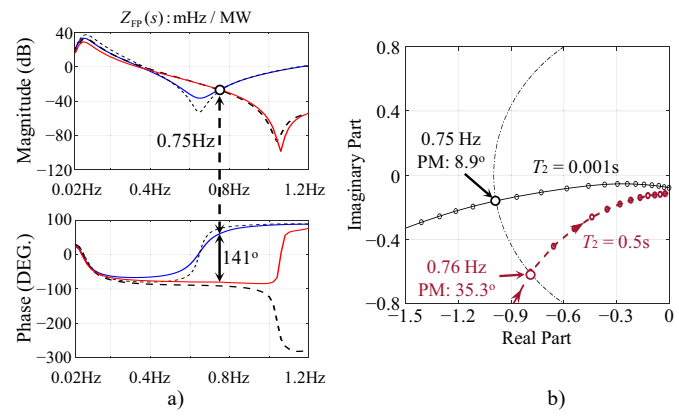


Fig. 7. Effect of increasing the governor lead time constant, T_2 , to 0.5s on the interarea mode of Kundur's two-area system. a) Analysis ignoring coupling effects using $Z_{\rm FP}(s)$ elements of the power-domain impedance; red lines: Area 1, blue lines: Area 2. Responses for the base case when T_2 is 0.001s are shown using black dashed lines. b) Analysis considering coupling using the Nyquist plot of the dominant eigenvalue of $\mathbf{Z}_1(s) \cdot \mathbf{Z}_2(s)^{-1}$; red lines: T_2 =0.5s, black lines: T_2 =0.001s (base case).

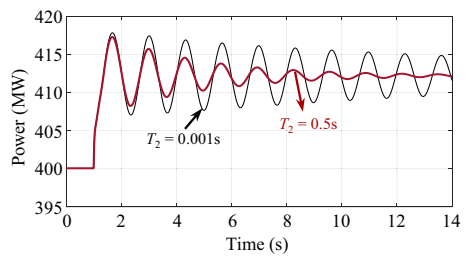


Fig. 8. Oscillations in the active power flow from Area 1 to Area 2 following a load transient when the governor lead-time constant T_2 is set at 0.001s (black thin lines) and when it is set at 0.5s (red thick lines).

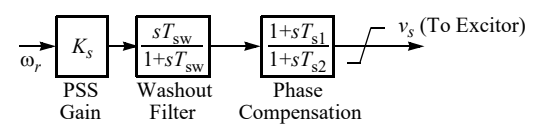


Fig. 9. PSS implementation in synchronous generators.

lead-time constant T_2 in all the generators is increased to 0.5s from 0.001s. Fig. 7a) shows the analysis ignoring the coupling effects, whereas Fig. 7b) shows the analysis considering the coupling effects. Both predict significant improvement in the phase margin of the 0.75 Hz mode; the phase margin prediction from Fig. 7a) is 39° (= 180° – 141°), whereas it is 35.3° from Fig. 7b). Simulated responses in Fig. 8 confirm the improvement in the damping after increasing the governor lead time constant from 0.001s to 0.5s.

Tuning of the governor time-constants may not be always feasible; the mainstream approach of damping power system oscillation modes is by using PSS in generators [7]. Fig. 9 shows a particular implementation of PSS used in this paper to demonstrate PSS design using the power-domain impedance method. It uses synchronous generator speed, ω_r , to create an auxiliary signal, v_s , that is added to the excitation system reference, as shown in Fig. 3b). The washout filter time constant $T_{\rm sw}$ in Fig. 9 is kept 10s, whereas the lead and lag time constants of the phase compensation, $T_{\rm s1}$ and $T_{\rm s2}$, are kept, 0.8s and 0.12s, respectively. The PSS gain, K_s , is used as a design parameter to provide

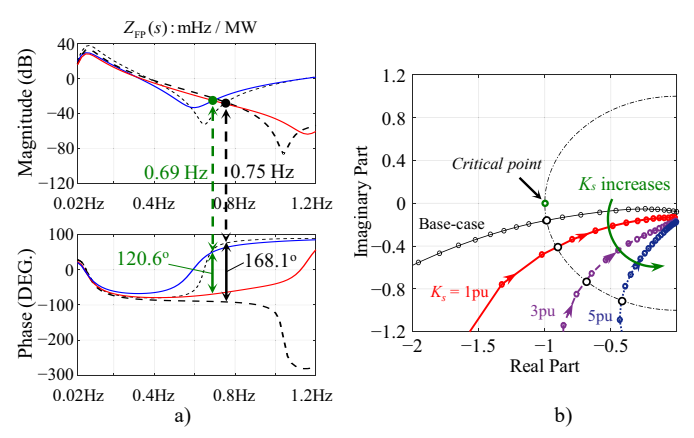


Fig. 10. Effect of PSS on the interarea mode of the two-area system. (a) Stability analysis ignoring coupling effects using the $Z_{\rm FP}(s)$ element of the power-domain impedance. Solid lines: with PSS, $K_s = 5$ pu (red lines: Area 1, blue lines: Area 2). Responses for the base case without PSS are shown using black dashed lines. (b) Stability analysis considering coupling elements using the Nyquist plot of the dominant eigenvalue of $\mathbf{Z}_1(s) \cdot \mathbf{Z}_2(s)^{-1}$; black line: base case (without PSS), red line: with PSS gain $K_s = 1$ pu, violet line: $K_s = 3$ pu, and blue line: $K_s = 5$ pu.

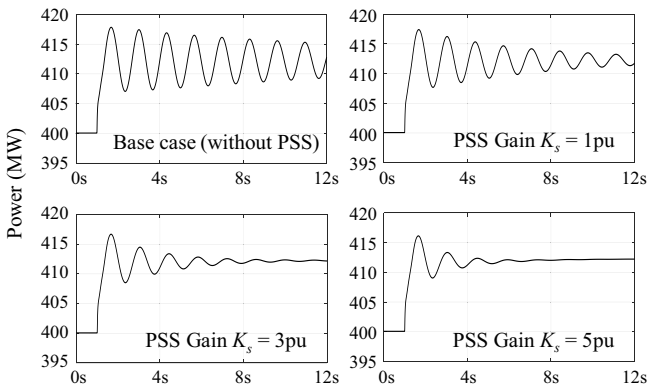


Fig. 11. Comparison of the response of the active power flow from Area 1 to Area 2 following a load transient for different PSS gains with the base case.

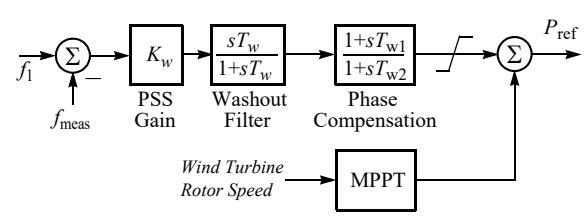


Fig. 12. PSS functionality in a wind power plant (Wind-PSS).

damping. Fig. 10 shows the power-domain impedance analysis for different values of the PSS gain. Fig. 10a) and b), which perform the analysis ignoring and considering the coupling elements, respectively, show progressive improvement in the damping of the interarea mode as the PSS gain is increased from 1 to 5 pu. Simulations in Fig. 11 confirm the progressive improvement in the damping of the interarea mode with the PSS gain.

C. Damping by a Wind Power Plant

This section demonstrates the design of PSS functionality in a 150 MW Type III wind power plant integrated at Bus 7 in the two-area system shown in Fig. 1. As shown in Fig. 12, an additional

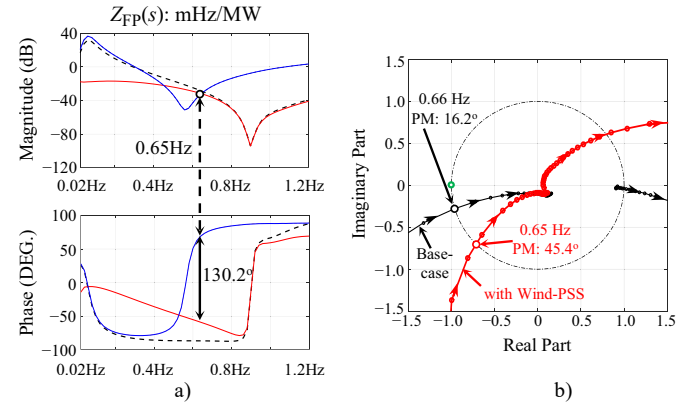


Fig. 13. Damping of the interarea mode by implementing PSS functionality in a wind power plant connected at Bus 7 in the two-area system. (a) Stability analysis ignoring coupling effects using the $Z_{\rm FP}(s)$ element of the power-domain impedance. Solid lines: with Wind-PSS (red lines: Area 1, blue lines: Area 2). Responses for the base case without Wind-PSS are shown using black dashed lines. (b) Analysis using the Nyquist plot of the dominant eigenvalue of $\mathbf{Z}_1(s)\cdot\mathbf{Z}_2(s)^{-1}$; black line: base case (without Wind-PSS), red line: with Wind-PSS

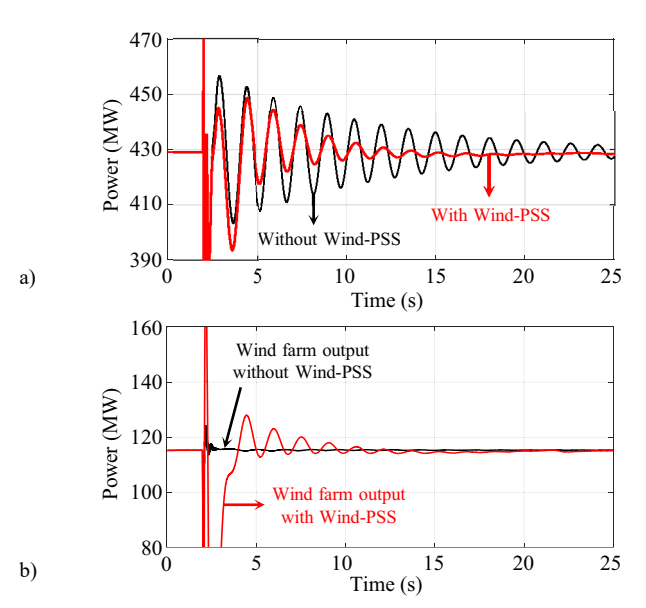


Fig. 14. Simulated responses following a transient fault event with and without PSS functionality by the wind power plant. a) active power flow from Area 1 to Area 2, and b) power output of the wind power plant.

power control loop is added in the wind turbines in parallel with the MPPT loop to modulate the active power output of the wind power plant depending on the error between the nominal frequency, f_1 , and the frequency measurement at the point of common coupling, f_{meas} . The power-domain impedance-based analysis of the system with and without the PSS functionality in the wind power plant is shown in Fig. 13; the analysis predicts significant improvement in the phase margin of the interarea mode after the installation of Wind-PSS in the wind power plant. The simulated responses in Fig. 14 confirm the improvement in the damping of the interarea mode using Wind-PSS. Note from Fig. 14b) how the wind power plant modulates its active power output after a transient transmission line fault to quickly damp the

interarea oscillations.

IV. CONCLUSIONS

Because of the use of non-standardized controls by IBR and unavailability of their dynamic models, new impedance-based tools are necessary for the stability analysis of modern power systems. The power-domain impedance theory presented in this paper can evaluate power system oscillations without depending on the analytical model of the system. Power-domain impedance responses can be measured at different points in the system using simulation models of the system or actual measurements. The power-domain impedance responses can be used both for predicting the power system oscillation modes as well as for designing damping controls in conventional generators and modern IBR including wind and PV power plants and inverterinterfaced energy storage systems. The online measurement of the power-domain impedance responses can also support the real-time monitoring of the power system frequency response [13] in addition to the power system oscillation modes.

REFERENCES

- [1] M. Singh, A. J. Allen, E. Muljadi, V. Gevorgian, Y. Zhang, and S. Santoso, "Interarea oscillation damping controls for wind power plants," *IEEE Trans. Sustain. Energy*, vol. 6, no. 3, pp. 967-975, July 2015.
- [2] L. Wu, S. You, X. Zhang, Y. Cui, Y. Liu, and Y. Liu, "Statistical analysis of the FNET/GridEye-detected inter-area oscillations in easter interconnection (EI)," in *Proc. 2017 Power and Energy Soc. Gen. Meeting*, Chicago, IL.
- [3] "Oscillation Event 03.12.2017 System Protection and Dynamics WG," ENTSO-E, Brussels, Belgium, 2018.
- [4] F. R. Schleif and J. H. White, "Damping for the northwest southwest oscillations—an analog study," *IEEE Trans. Power App. and Syst.*, vol. 85, no. 12, pp. 1239-1247, Dec. 1966.
- [5] W. Mo, Y. Chen, H. Chen, Y. Liu, Y. Zhong, J. Hou, Q. Gao, and C. Li, "Analysis and measures of ultralow-frequency oscillations in a large-scale hydropower transmission system," *IEEE. J. Emerg. Sel. Topics Power Electron.*, vol. 6, no. 3, pp. 1077-1085, Se. 2018.
- [6] P. Kundur, Power System Stability and Control. McGraw-Hill, 1994.
- [7] F. P. Demello and C. Concordia, "Concepts of synchronous machine stability as affected excitation control," *IEEE Trans. Power App. and Syst.*, vol. 88, no. 4, pp. 316-329, April 1969.
- [8] E. Rehman, M. Miller, J. Schmall, S. H. Huang, "Dynamic stability assessment of high penetration of renewable generation in the ERCOT grid," ERCOT, Taylor, TX, USA, 2018. [Online]. http://www.ercot.com/ content/wcm/lists/144927/Dynamic_Stability_Assessment_of_High_Penetration_of_Renewable_Generation.pdf
- [9] E. Rehman, M. G. Miller, J. Schmall, S. H. Huang, and J. Billo, "Stability assessment of high penetration of inverter-based generation in the ERCOT grid," in *Proc. 2019 IEEE Power and Energy Soc. Gen. Meeting*, Atlanta, GA.
- [10] J. F. Hauer, "Application of prny analysis to the determination of modal content and equivalent modes! for measured power system responses," *IEEE Trans. Power Syst.*, vol. 6, no. 3, pp. 1062-1068, Aug. 1991.
- [11] S. Shah and L. Parsa, "Impedance modeling of three-phase voltage source converters in DQ, sequence, and phasor domains," *IEEE Trans. Energy Conv.*, vol. 32, no. 3, pp. 1139-1150, April 2017.
- [12] S. Shah, "Small and large signal impedance modeling for stability analysis of grid-connected voltage source converters," Ph.D. dissertation, Dept. Elect. Eng., Rensselaer Polytechnic Institute, Troy, NY, 2018.
- [13] S. Shah and V. Gevorgian, "Impedance-based characterization of power system frequency response," in *Proc. 2019 Power and Energy Soc. Gen. Meeting (PESGM)*, Atlanta, GA.